Supporting Information

van Dooren *et al.* 10.1073/pnas.0803862105

SI Materials and Methods

Gene Cloning and Sequence Analyses. We used sequence from a Tic20 homolog from the red alga *Cyanidioschyzon merolae* [CMS050C (1)] as a query for an iterative PSI-BLAST search (2) against a nonredundant protein sequence database (ncbi.nlm-.nih.gov/blast/Blast.cgi). After two iterations using default parameters, we identified a hit to genes from *Theileria* species and used these as query sequences to identify Tic20 homologs in other Apicomplexa. We identified one predicted gene in *Toxoplasma gondii* with homology to the *Theileria* genes. An EST covered the 3′ end of this gene. To identify the 5′ end, we performed 5′ RACE by using the SMART RACE cDNA amplification kit (BD Biosciences), with the initial primer 5′-TTGAGATATATCATGCTCA and the nested primer 5′-AGCATAGACAGTAGCAAA. Sequencing of the entire *Tg*Tic20 gene revealed the presence of three introns and an ORF of 1,170 bp. The GenBank accession number for *Tg*Tic20 is EU427503. To compare *Tg*Tic20 with other known Tic20 homologs we generated a multiple sequence alignment as described in ref. 3. Other sequences included in the alignment were identified from publicly available databases.

Plasmid Construction, Parasite Transfection, and Parasite Culture. The ORF of *Tg*Tic20 was amplified by PCR using the primers 5′-AGATCTAAAATGGGGTTCCCTTCAGCTCTCT and 5′-CCTAGGGTACGAGTCTGACGGCTTCTCGCCGAT. The resultant PCR product was subcloned into pCR2.1 (Invitrogen) and verified by sequencing. The resulting vector was digested with BglII and AvrII and cloned into the equivalent sites of the pCTH vector (G.G.v.D. and R. Opperman, unpublished data) to generate pCTH(Tic20). This vector contains the Tic20 ORF downstream of the *T. gondii* α-tubulin promoter, with a 3′ HA tag fusion and a chloramphenicol resistance marker for selection in *T. gondii*. This was transfected into RH strain *T. gondii* parasites as described in ref. 4. Stable lines expressing the tub-*Tg*Tic20-HA construct were generated by chloramphenicol selection (5).

To generate a conditional knockout of *Tg*Tic20, we first generated a parental strain that expressed inducible copies of *Tg*Tic20. To do this, we placed the *Tg*Tic20 ORF into the BglII- and AvrII-cut sites of pDt7s4M vector (G.G.v.D., unpublished data), which contains a mutant form of dihydrofolate reductase (DHFR) that encodes resistance to pyrimethamine, an inducible teto7/sag4 promoter, and a c-myc tag at the 3′ end of the gene of interest. We transfected the resulting construct into TATi strain *T. gondii* parasites, containing a transactivating tetracycline repressor protein to enable inducible repression of *Tg*Tic20-c-myc gene expression (6). We then proceeded to knock out endogenous *Tg*Tic20 through double homologous recombination. We amplified ≈2 kb downstream of the *Tg*Tic20 protein-coding sequences with the primers 5′-AAGCTTACAAGTTG-CAGTAGGTGTTCCA and 5′-CTCGAGAAGCAGTGT-GGTCGAAAGATA and placed this into the HindIII- and XhoI-cut sites of the vector pTCY (G.G.v.D., unpublished data). pTCY is a modified version of the ptubCAT vector (a kind gift from Markus Meissner, University of Heidelberg, Heidelberg, Germany), containing a chloramphenicol resistance marker driven by the tubulin promoter and containing multicloning sites flanking both sides of the expression cassette. This vector also contains a yellow fluorescent protein (YFP) marker for negative selection of successful homologous recombinants (7). We amplified ≈2 kb upstream of the *Tg*Tic20 protein coding sequence with the primers 5′-ACTAGTAACAGCGCTGTCTC-CCCCATAA and 5′-AGATCTTTTCCTCGAGGCAGTAG-TATA and ligated this into the SpeI- and BglII-cut sites of the pTCY(Tic20 3′) vector. This generated the vector pTCY(Tic20 KO). We linearized this plasmid with NotI and transfected it into the parental strain and selected on chloramphenicol. After obtaining chloramphenicol-resistant parasites, we cloned YFP-negative parasites by cell sorting as described previously (7). We isolated 16 clones and performed diagnostic PCR and Southern blotting (see below) to identify successful targeting of the *Tg*Tic20 locus.

To complement the *Tg*Tic20 knockout, we expressed a tub-*Tg*Tic20-HA plasmid containing a phleomycin resistance cassette in the knockout parasite line. We generated this vector by digesting the phleomycin resistance cassette of the pBSSK$^+$ SAG1/Ble/SAG1 (a gift from David Sibley, Washington University, St. Louis, MO) with HindIII and SpeI and ligated this into the equivalent sites of pCTH(Tic20) to generate the vector pBTH(Tic20). We transfected this into the *Tg*Tic20-knockout cell line and selected for parasites stably expressing the complemented *Tg*Tic20-HA construct by phleomycin selection as described in ref. 8.

To generate *Tg*Tic20 parental, mutant, and complemented cell lines expressing tandem tomato RFP parasites, we amplified tandem dimeric tomato sequence (9) by using the primers 5′-AGTCCCTAGGGTGAGCAAGGGCGAGGAG and 5′-AGTCCCCGGGCTTGTACAGCTCGTCCATGC. We digested the resulting PCR product with AvrII and XmaI and ligated it into the equivalent sites of pCTG (G.G.v.D. and R. Opperman, unpublished data). This generated the vector $pCTR_{2T}$, containing the tandem dimeric tomato RFP expressed from the tubulin promoter. We transfected this construct into the various cell lines and subjected parasites to three or four rounds of cell sorting before cloning. Cell sorting was performed by using a MoFlo sorter (Dako), with an Enterprise 621 laser tuned to 488 nm. We sorted cells expressing tomato parasites by using a 570/40 nm BP filter.

To generate vectors for the split GFP system (10), we amplified GFP 1–10 with the primers 5′-AGTCCCTAGGAG-CAAAGGAGAAGAACTTTT and 5′-AGTCCCCGGGT-TAGGTACCCTTTTCGTTGGGATCT and GFP-11 with the primers 5′-AGTCCCTAGGGGTTCCGATGGAGGGTCT-GGTG and 5′-AGTCCCCGGGTTATGTAATCCCAGCAG-CATT (parent vectors were gifts from Geoff Waldo, Los Alamos National Research Laboratory, Los Alamos, NM). We digested the resultant PCR products with AvrII and XmaI and ligated these into the equivalent sites of the pCTG vector to make the vectors $pCTG_{1–10}$ and $pCTG_{11}$. We digested the ferredoxin-NAPD$^+$ reductase (FNR) leader sequence from the ptubFNR-RFP/sagCAT vector (11) and the P30 sequence from the ptubP30-GFP/sag-CAT vector (12) with BglII and AvrII, ligated these into equivalent sites in the $pCTG_{1–10}$ vector, and transfected RH strain *T. gondii* parasites. Parasites stably expressing FNR-GFP 1–10 and P30-GFP 1–10 were obtained through chloramphenicol selection. The entire *T. gondii* acyl carrier protein (ACP)-coding region was digested from the vector ptubACPfull-GFP/sag-CAT (13) with BglII and AvrII and ligated into equivalent sites of $pCTG_{11}$. The result vector was transfected into the cell line stably expressing FNR-GFP 1–10 and fluorescent parasites obtained through several rounds of cell sorting by using a MoFlo flow cytometer (Dako) with an Enterprise 621 laser tuned to 488 nm by using a 530/40 nm BP

filter. P30 and the complete Tic20 ORF were digested from the ptubP30-GFP/sag-CAT and pCTH(Tic20) vectors with BglII and AvrII and ligated into the equivalent sites of $pCTG_{11}$. The chloramphenicol resistance cassette of $pCTG_{11}$(P30) was replaced with a DHFR cassette encoding resistance to pyrimethamine by digestion of the pKOsagDHFR vector (a gift from Marc-Jan Gubbels, Boston College, Boston, MA) with HindIII and SpeI and ligation into the equivalent sites of $pCTG_{11}$(P30). The resultant construct was transfected into the FNR-GFP 1–10 cell line and selected on pyrimethamine as described in ref. 14 and cloned by limiting dilution. The chloramphenicol resistance cassette of $pCTG_{11}$(Tic20) was replaced with a BLE cassette encoding resistance to phleomycin by digestion of the $pBSSK^+$ SAG1/Ble/SAG1 vector with HindIII and SpeI and ligation into equivalent sites of $pCTG_{11}$(Tic20). The resultant $pBTG_{11}$(Tic20) vector was transfected into the parasite line expressing FNR-GFP 1–10, selected on phleomycin, and cloned by limiting dilution. Fluorescence intensities were quantified by flow cytometry by using a MoFlo cytometer as described above, and results were analyzed and graphed used FlowJo software (Tree Star).

To generate a cell line expressing both tub-*Tg*Tic20-HA and APT1-YFP, we made a plasmid expressing APT1-YFP containing a phleomycin-selectable marker. We digested pBTH(Tic20) and an APT1-YFP vector (a gift from Manami Nishi and David Roos, University of Pennsylvania, Philadelphia, PA) with BglII and NotI and ligated APT1-YFP into the equivalent sites of the pBT vector. We transfected this construct into the cell line expressing tub-*Tg*Tic20-HA and generated parasites stably expression APT1-YFP by phleomycin selection.

To generate a construct that targeted mouse DHFR fused to a C-terminal HA tag to the apicoplast, we digested the FNR leader sequence from the ptubFNR-RFP/sagCAT vector (11) with BglII and AvrII and ligated this into the equivalent sites of pCTH. We then amplified mouse DHFR from cDNA (a gift from Jörn Lakowski, University of Georgia, Athens, GA) with the primers 5′-CCTAGGGGTGGAAGCATGGTTCGACCATTGAACTGC and 5′-ACTAGTGTCTTTCTTCTCGTAGACTT. Mouse DHFR was digested with AvrII and SpeI and ligated into the AvrII site of pCTH(FNR). We replaced the chloramphenicol resistance cassette with a phleomycin resistance cassette and transfected the resultant pBTH(FNR-mDHFR) vector into the *Tg*Tic20 knockout and parental lines. Stable parasites expressing this construct were obtained through phleomycin selection.

To generate *Tg*Tic20 knockout and parental cell lines expressing apicoplast-targeted RFP, we digested the ptubFNR-RFP/sagCAT vector with BglII and NotI and ligated this into the equivalent sites of pBTH(Tic20). We transfected the resultant pBTR(FNR) construct into the *Tg*Tic20 knockout and parental lines and obtained stable expressors through phleomycin selection.

Parasite Growth Assays. To measure parasite growth we performed plaque assays by adding 400 parasites to a T25 flask containing a confluent monolayer of human foreskin fibroblasts. We grew parasites undisturbed for 9 days, washed once with PBS [0.8% (wt/vol) NaCl, 0.02% (wt/vol) KCl, 0.14% (wt/vol) Na_2HPO_4, 0.02% KH_2PO_4, pH 7.4], fixed the monolayer with ethanol, and stained with 2% (wt/vol) crystal violet in a solution of 20% (vol/vol) ethanol and 0.8% (wt/vol) ammonium oxalate. Tandem tomato RFP fluorescence plate assays were performed essentially as described in ref. 15. Human foreskin fibroblast cells were grown to confluence in 96-well Costar optical bottom plates (Corning). We seeded 4,000 parasites per well and measured tomato fluorescence daily by using a SpectraMax $M2^e$ microplate reader (Molecular Devices). Readings were taken from the bottom, by using a 544-nm excitation and a 590-nm emission wavelength with a 570-nm cutoff. Percent positivity values were derived as described in ref. 15.

Western Blotting and Detection of Membrane Proteins. Protein samples (typically to a cell equivalent of 5×10^6 parasites) were loaded onto precast 12% Bis-Tris and 3–8% Tris-acetate NuPAGE gels (Invitrogen). After separation by electrophoresis, proteins were transferred to nitrocellulose membrane. Blots were probed with antibodies against ACP [1:1,000 to 1:2,000 dilution; a gift from Geoff McFadden, University of Melbourne, Victoria, Australia (13)], GRA8 [1:200,000; a gift from Gary Ward, University of Vermont, Burlington, VT (16)], anti-HA (1:100 to 1:500, clone 3F10; Roche Applied Science), anti c-myc (1:50 to 1:100, clone 9E10; Roche Applied Science), and anti-GFP (1:1,00; Torry Pines Biolabs). Horseradish peroxidase (HRP)-conjugated anti-rat and anti-rabbit antibodies (Pierce) were used at 1:5,000 to 1:10,000 dilutions, although HRP-conjugated anti-mouse antibodies (TrueBlot; eBioscience) were used at 1:1,000 dilution.

Membrane proteins were identified by alkaline (sodium carbonate) extractions and by Triton X-114 phase partitioning. For alkaline extractions (17), parasite pellets were washed once in PBS then incubated in 100 mM sodium carbonate (pH 11.5 or 12.5) for 30 min on ice. Samples were centrifuged at 150,000 × *g* at 4°C for 45 min. Pellets (containing integral membrane proteins) were resuspended in sample buffer, whereas supernatant proteins were precipitated by trichloroacetic acid before resuspension in sample buffer. Triton X-114 partitioning was performed as described in refs. 18 and 19. Briefly, parasite pellets were resuspended in PBS containing 1% (vol/vol) Triton X-114, 2 mM EDTA, and supplemented with protease inhibitors (Complete protease inhibitor mixture; Roche). Cells were incubated on ice for 30 min and centrifuged to remove insoluble material. The supernatant was layered onto a sucrose cushion (6% sucrose, 0.06% Triton X-114 in PBS) and incubated at 37°C for 3 min. The sample was centrifuged for 2 min at room temperature, and the layer above the cushion (containing soluble-phase proteins) was subjected to trichloroacetic acid precipitation before resuspension in sample buffer. The detergent micelles below the sucrose cushion (containing membrane proteins) were also extracted, resuspended in cold PBS, and subjected to trichloracetic acid precipitation before resuspension in sample buffer. Proteins were separated by SDS/PAGE and detected by Western blotting (see above).

Pulse–Chase and Immunoprecipitation. Confluent T25 flasks were infected with $\approx 2 \times 10^6$ parasites and allowed to grow for 2 days. Infected host cells were starved for 1 h in cysteine and methionine-free Dulbecco's modified Eagle's medium supplemented with 1% dialyzed fetal bovine serum and antibiotics. Infected host cells were radiolabeled with 100 μCi/ml [^{35}S]methionine/cysteine (GE Healthcare) for 1 h. Cells were either harvested (pulse) or washed twice with 10 ml of parasite growth medium, and incubated in 10 ml of parasite growth medium for 2 h (chase) before harvesting. Proteins of interest were purified by immunoprecipitation or affinity purification (see below) and separated by SDS/PAGE as described above. Gels were dried, and bands were visualized by autoradiography or by using a Storm 860 PhosphorImager (GE Healthcare). Band intensities were quantified by using ImageQuant TL software (GE Healthcare).

For immunoprecipitations, parasites were lysed from host cells by passage through a 26-gauge needle and pelleted by centrifugation at 1,500 × *g* for 10 min. Pellets were washed in PBS and then lysed for 30 min on ice in immunoprecipitation lysis buffer [50 mM Tris·HCl (pH 8.0), 150 mM NaCl, 1% (vol/vol) Nonidet P-40 substitute (Fluka), 0.5% (wt/vol) sodium deoxycholate, 0.1% (wt/vol) SDS, 2 mM EDTA] supplemented with protease inhibitors. Samples were centrifuged to remove insoluble mate-

rial. Proteins of interest were purified by immunoprecipitation using anti-HA-conjugated agarose beads (Roche Applied Science), anti-c-myc-conjugated agarose beads (Santa Cruz Biotechnology), or antibodies bound specifically to protein A–Sepharose CL-4B beads (GE Healthcare). For the latter application, samples were precleared by incubation in 30–40 μl of a 50% slurry of protein A–Sepharose CL-4B beads. Antibodies including MIC5 [a gift from Vern Carruthers, University of Michigan, Ann Arbor (20)], anti-lipoic acid (Calbiochem), and anti-ACP were bound to protein A–Sepharose CL-4B beads for 1 h at 4°C before addition to precleared lysates. All samples were incubated overnight at 4°C and then washed four times in immunoprecipitation wash buffer [50 mM Tris·HCl (pH 8.0), 150 mM NaCl, 1% (vol/vol) Nonidet P-40 substitute, 0.5% (wt/vol) sodium deoxycholate, 0.25% (wt/vol) BSA, 2 mM EDTA] and twice in PBS. Samples were eluted by boiling in reducing or nonreducing sample buffer then separated by SDS/PAGE as described above. For affinity purification of biotinylated proteins, lysates were incubated overnight with immobilized streptavidin–agarose beads (Pierce). Samples were washed four times in streptavidin wash buffer [50 mM Tris·HCl (pH 8.0), 150 mM NaCl, 1% (vol/vol) Nonidet P-40 substitute, 0.5% (wt/vol) sodium deoxycholate, 0.1% (wt/vol) SDS, 2 mM EDTA] and twice in PBS before elution by boiling in reducing sample buffer.

Southern Blotting. Genomic DNA was extracted from parasite strains by using the DNeasy kit (Qiagen). Two micrograms was digested overnight with KpnI and separated by electrophoresis on a 0.8% agarose gel. Gels were treated with 0.2 M HCl for 15 min, denatured in 1.5 M NaCl and 0.5 M NaOH for 30 min, and neutralized for 40 min in 1.5 M NaCl and 1 M Tris (pH 8.0). DNA was capillary-transferred onto Nytran SuPerCarge nylon membrane (Schleicher & Schuell) overnight in 20× SSPE buffer [3 M NaCl, 20 mM EDTA, 0.2 M sodium phosphate (pH 7.4)], then cross-linked by using a CL-1000 UV cross-linker (UVP). The membrane was prehybridized for 4 h at 42°C in 40% (vol/vol) formamide, 1.25 × SSPE, 0.625% (wt/vol) SDS, Denhardt's solution [0.02% (wt/vol) Ficoll, 0.02% (wt/vol) polyvinylpyrrolidone, 0.02% (wt/vol) BSA] and 10% (wt/vol) dextran sulfate. A probe against *Tg*Tic20 was amplified from genomic DNA by using the same primers as for amplifying the entire ORF (above). The probe was radiolabeled with [^{32}P]dATP by using the random primers DNA labeling system (Invitrogen) according to the manufacturer's instructions and hybridized to the nylon membrane overnight at 42°C. The membrane was washed three times in 2× SSPE for 15 min at room temperature, three times in 2× SSPE containing 1% (wt/vol) SDS for 15 min at 42°C, and rinsed a further two times in 2× SSPE. Bands were detected by exposure to autoradiography film.

Microscopy. Light microscope images were taken with a DM IRBE inverted epifluorescence microscope (Leica) fitted with a 100× oil immersion objective lens (PL APO 1.40 NA). Images were recorded by using a Hamamatsu C4742–95 digital camera and adjusted for brightness and contrast using Openlab software (Improvision). Live imaging was performed on infected coverslips in a sealed chamber at room temperature. For immunofluorescence, we fixed infected coverslips in 3% paraformaldehyde for 15 min, permeabilized in 0.25% Triton X-100 for 10 min, then blocked in 2% (wt/vol) BSA for 30 min. Samples were labeled with primary antibody for 1 h, washed three times in PBS, incubated in secondary antibody for a further hour, and washed three times in PBS. Primary antibodies used were rabbit anti-ACP (1:1,000 to 1:2,000 dilution) and rat anti-HA (1:100 to 1:500). Secondary antibodies used were goat anti-rabbit Alexa Fluor 546 (1:500) and goat anti-rat Alexa Fluor 488 (1:200; Molecular Probes).

For electron microscopy, flasks containing confluent human foreskin fibroblast cells were infected with the tub*Tg*Tic20-HA strain of *T. gondii*. Cryosectioning was done according to refs. 21–23. Cells were fixed for 24 h in 2% formaldehyde and 0.2% glutaraldehyde in 0.1 M phosphate buffer and subsequently embedded in 12% gelatin in phosphate buffer. The gelatin-embedded cells were cut in cubes and infiltrated with 2.3 M sucrose for 10–20 h at 4°C. Samples were mounted on a sample holder, frozen in liquid nitrogen, and cryosectioned by using cryoultramicrotome UCT/FCS (Leica Microsystems). The cryosections were picked up with a drop of 1% methyl cellulose and 1.15 M sucrose in PBS (24) and transferred to Formvar carbon-coated hexagonal 200 mesh grids. The grids with ultrathin sections were washed for 30 min at 37°C in phosphate buffer (pH 7.4) and blocked for 15 min on drops of PBS containing 1% BSA and 0.05% cold water fish skin gelatin (Sigma). The grids were incubated for 60 min with anti-HA antibody (12CA5; Roche), rinsed in PBS containing 0.1% BSA and 0.005% cold water fish skin gelatin, and incubated for 20 min with a bridging rabbit anti-mouse antibody (DakoCytomation). After the second washing step, the grids were incubated for 20 min with protein A coupled to gold (PAG, 10 nm; Utrecht University, The Netherlands). The label was fixed onto the cryosections with 1% glutaraldehyde in PBS for 5 min. For double labeling, the cryosections were subsequently blocked as described above, then incubated for 60 min with anti-ACP antibody, rinsed, and incubated for 20 min with PAG for 15 nm. The grids were fixed for 5 min in 1% glutaraldehyde in PBS and rinsed in distilled water for 10 min. Cryosections were poststained with 2% uranyl acetate in 0.15 M oxalic acid [pH 7.4 (22)] and embedded in 1.8% methyl cellulose containing 0.4% aqueous uranyl acetate. Grids were examined in a transmission electron microscope (Tecnai 12; FEI Company) at 120 kV. Images were recorded by using a CCD camera (MegaView II; Soft Imaging Systems). Image processing was done with Analysis 3.2 (Soft Imaging Systems).

1. Matsuzaki M, *et al.* (2004) Genome sequence of the ultrasmall unicellular red alga *Cyanidioschyzon merolae* 10D. *Nature* 428:653–657.
2. Altschul SF, *et al.* (1997) Gapped BLAST and PSI-BLAST: A new generation of protein database search programs. *Nucleic Acids Res* 25:3389–3402.
3. Gubbels MJ, Vaishnava S, Boot N, Dubremetz JF, Striepen B (2006) A MORN-repeat protein is a dynamic component of the. *Toxoplasma gondii* cell division apparatus. *J Cell Sci* 119:2236–2245.
4. Striepen B, Soldati D (2007) *Toxoplasma gondii. The Model Apicomplexan*: *Perspectives and Methods*, eds Weiss LD, Kim K (Elsevier, London), pp 391–415.
5. Kim K, Soldati D, Boothroyd JC (1993) Gene replacement in *Toxoplasma gondii* with chloramphenicol acetyltransferase as selectable marker. *Science* 262:911–914.
6. Meissner M, Schluter D, Soldati D (2002) Role of *Toxoplasma gondii* myosin A in powering parasite gliding and host cell invasion. *Science* 298:837–840.
7. Mazumdar J, Wilson EH, Masek K, Hunter CA, Striepen B (2006) Apicoplast fatty acid synthesis is essential for organelle biogenesis and parasite survival in *Toxoplasma gondii. Proc Natl Acad Sci USA* 103:13192–13197.
8. Messina M, Niesman I, Mercier C, Sibley LD (1995) Stable DNA transformation of *Toxoplasma gondii* using phleomycin selection. *Gene* 165:213–217.
9. Shaner NC, *et al.* (2004) Improved monomeric red, orange, and yellow fluorescent proteins derived from *Discosoma* sp. red fluorescent protein. *Nat Biotechnol* 22:1567–1572.
10. Cabantous S, Terwilliger TC, Waldo GS (2005) Protein tagging and detection with engineered self-assembling fragments of green fluorescent protein. *Nat Biotechnol* 23:102–107.
11. Striepen B, *et al.* (2000) The plastid of *Toxoplasma gondii* is divided by association with the centrosomes. *J Cell Biol* 151:1423–1434.
12. Striepen B, He CY, Matrajt M, Soldati D, Roos DS (1998) Expression, selection, and organellar targeting of the green fluorescent protein in *Toxoplasma gondii. Mol Biochem Parasitol* 92:325–338.
13. Waller RF, *et al.* (1998) Nuclear-encoded proteins target to the plastid in T*oxoplasma gondii* and *Plasmodium falciparum. Proc Natl Acad Sci USA* 95:12352–12357.
14. Donald RG, Roos DS (1993) Stable molecular transformation of. *Toxoplasma gondii*: A selectable dihydrofolate reductase–thymidylate synthase marker based on drug-resistance mutations in malaria. *Proc Natl Acad Sci USA* 90:11703–11707.
15. Gubbels MJ, Li C, Striepen B (2003) High-throughput growth assay for *Toxoplasma gondii* using yellow fluorescent protein. *Antimicrob Agents Chemother* 47:309–316.

16. Carey KL, Donahue CG, Ward GE (2000) Identification and molecular characterization of GRA8, a novel, proline-rich, dense granule protein of. *Toxoplasma gondii. Mol Biochem Parasitol* 105:25–37.
17. Fujiki Y, Hubbard AL, Fowler S, Lazarow PB (1982) Isolation of intracellular membranes by means of sodium carbonate treatment: Application to endoplasmic reticulum. *J Cell Biol* 93:97–102.
18. Bordier C (1981) Phase separation of integral membrane proteins in Triton X-114 solution. *J Biol Chem* 256:1604–1607.
19. Mullin KA, *et al.* (2006) Membrane transporters in the relict plastid of malaria parasites. *Proc Natl Acad Sci USA* 103:9572–9577.
20. Brydges SD, *et al.* (2000) Molecular characterization of TgMIC5, a proteolytically processed antigen secreted from the micronemes of. *Toxoplasma gondii. Mol Biochem Parasitol* 111:51–66.
21. Tokuyasu KT (1973) A technique for ultracryotomy of cell suspensions and tissues. *J Cell Biol* 57:551–565.
22. Tokuyasu KT (1978) A study of positive staining of ultrathin frozen sections. *J Ultrastruct Res* 63:287–307.
23. Tokuyasu KT (1980) Immunochemistry on ultrathin frozen sections. *Histochem J* 12:381–403.
24. Liou W, Geuze HJ, Slot JW (1996) Improving structural integrity of cryosections for ImmunoGold labeling. *Histochem Cell Biol* 106:41–58.
25. Armbrust EV, *et al.* (2004) The genome of the diatom *Thalassiosira pseudonana*: Ecology, evolution, and metabolism. *Science* 306:79–86.

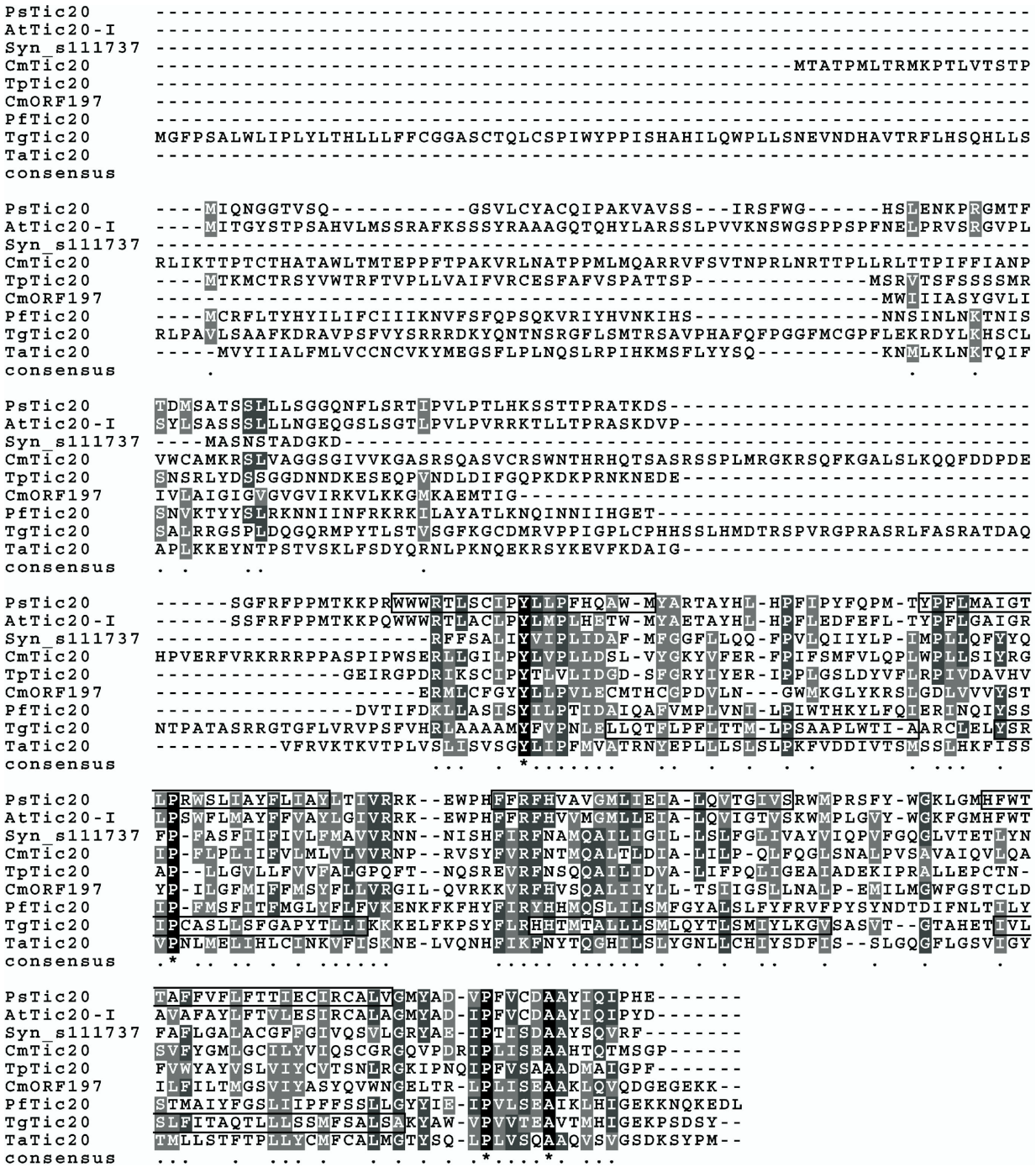

Fig. S1. Multiple sequence alignment of Tic20 protein homologs. The alignment includes Tic20 homologs from the plants *Pisum sativum* (PsTic20; GenBank accession number AAC64607) and *Arabidopsis thaliana* (AtTic20-I; NP_171986), the cyanobacterium *Synechocystis* species PCC 6803 (Syn_sll1737; NP_440747), the red alga *Cyanidioschyzon merolae* nuclear-encoded [CmTic20; genome accession number CMS050C, *http://merolae.biol.s.u-tokyo.ac.jp/* (1)] and *C. merolae* plastid-encoded (CmORF197; CMV078C), the diatom *Thalassiosira pseudonana* [TpTic20; gene model predicted by authors based on sequence available at genome website: *http://genome.jgi-psf.org/Thaps3/Thaps3.home.html*; (25)], and the Apicomplexa *T. gondii* (TgTic20; this study; EU427503), *Theileria annulata* (TaTic20; XP_951914), and *Plasmodium falciparum* (PfTic20; AAN36039). Conserved and similar residues with an identity threshold of 0.60 are shaded and marked by asterisks and dots on the consensus line. The boxed regions in the PsTic20 and TgTic20 sequences represent predicted transmembrane domains (based on TMHMM Server predictions; www.cbs.dtu.dk/services/TMHMM/).

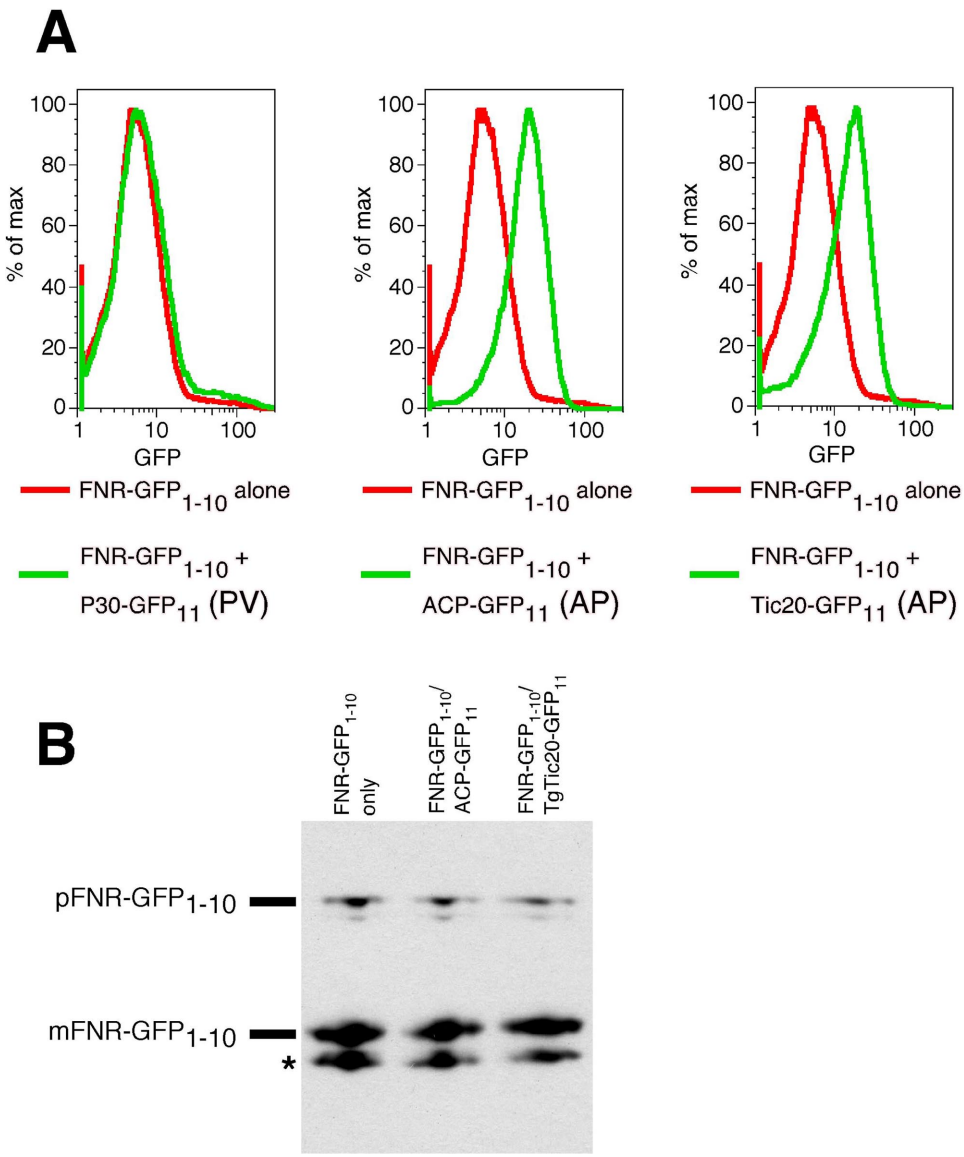

Fig. S2. Quantification of split-GFP experiments. (*A*) To quantify fluorescence levels, cell strains depicted in Fig. 2, in addition to cell strains expressing FNR-GFP 1–10 alone and FNR-GFP 1–10 with P30-GFP-11, were analyzed by flow cytometry. When the split GFP molecules are targeted to separate compartments of the secretory pathway (*Left*, green line), fluorescence intensity equates to that of FNR-GFP 1–10 alone (red line on all graphs). Fluorescence intensities in strains coexpressing FNR-GFP 1–10 with either ACP-GFP-11 (*Center*, green line) or *Tg*Tic20-GFP-11 (*Right*, green line) are considerably greater than in FNR-GFP 1–10 alone. (*B*) Western blot of parasite cell lines containing either FNR-GFP 1–10 alone or coexpressed with ACP GFP-11 or *Tg*Tic20 GFP-11. The anti-GFP antibody labels GFP 1–10 alone. Each cell line contains low levels of precursor FNR-GFP 1–10, with most GFP 1–10 existing in the mature, processed form, suggesting that in each cell line, most GFP 1–10 reaches the apicoplast stroma. Asterisk labels a possible GFP 1–10 degradation product, similar to those observed for apicoplast-targeted GFP molecules (13).

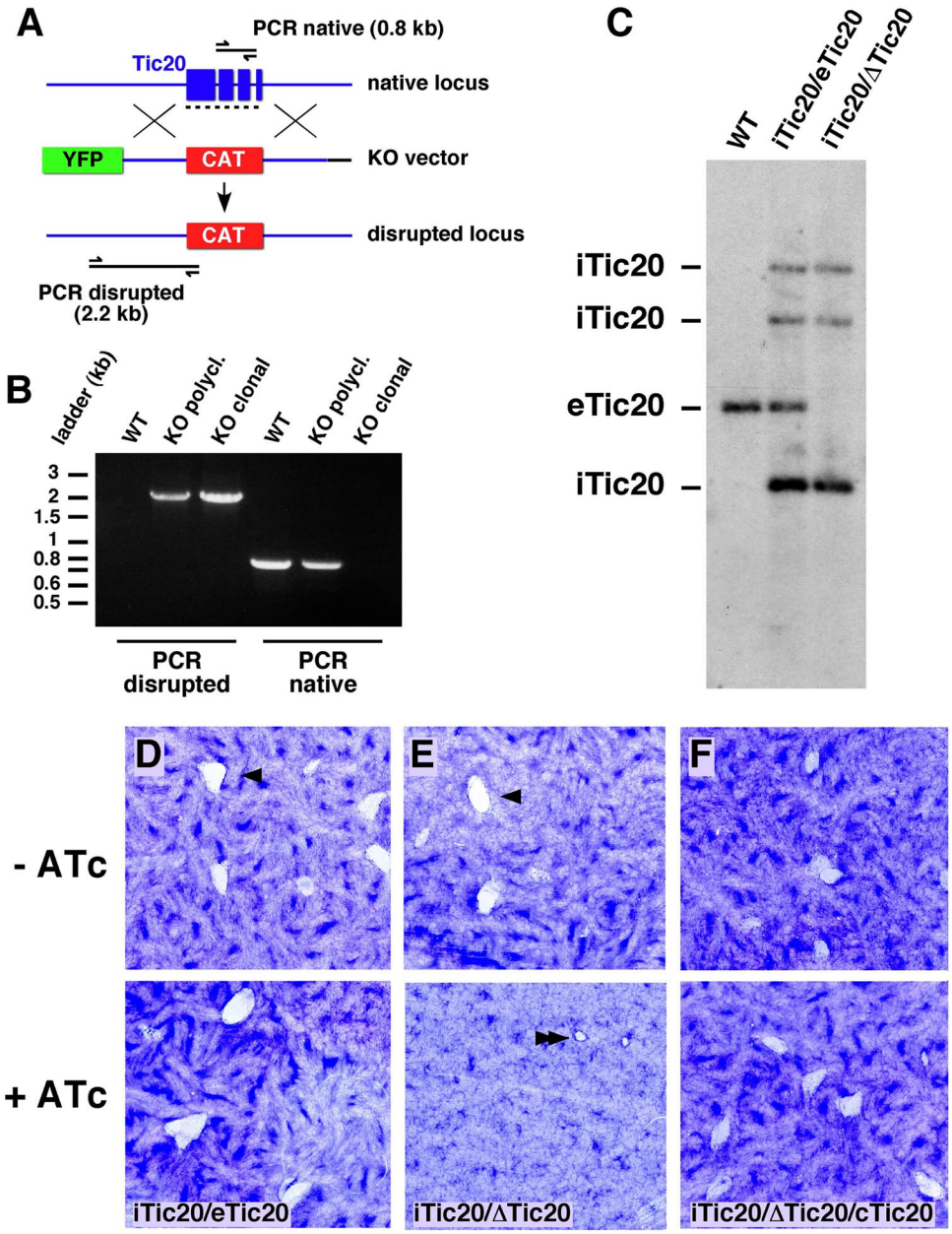

Fig. S3. Genetic disruption of *Tg*Tic20. (*A*) Schematic depicting genetic disruption of the native TgTic20 locus. We generated a knockout construct (KO vector) containing a chloramphenicol acetyltransferase (CAT) gene flanked by 2-kb sequences homologous to the 5′ and 3′ flanks of the native *Tg*Tic20 locus. A YFP marker for negative selection is located outside this knockout cassette. We transfected linearized knockout vector into a parasite cell line expressing inducible copies of *Tg*Tic20, selected for CAT-resistant parasites, and then further selected for homologous integrants through fluorescence sorting of parasites not expressing YFP. (*B*) We performed diagnostic PCR analysis to verify disruption of the *Tg*Tic20 locus. One set of PCR primers was specific for the disrupted *Tg*Tic20 locus (PCR disrupted), and a second set was designed within introns of the *Tg*Tic20 gene and is thus specific to the native locus (PCR native). We observed a PCR product of the predicted size for the native gene in wild-type (WT) parasites but not in knockout parasite clones (KO clonal). Conversely, we observed a PCR product of the predicted size for the disrupted gene in clonal knockout but not in wild-type parasites. (*C*) We performed Southern blotting on RH strain WT, parental (iTic20/eTic20), and knockout (iTic20/ΔTic20) parasites by using a probe against the entire *Tg*Tic20 gene. A band the expected size for the endogenous gene (eTic20) is expressed in both WT and parental parasites but not in knockout parasites. Extra bands in the parental and knockout strains represent introduced inducible copies of the *Tg*Tic20 gene (iTic20). (*D–F*) To measure the effects of *Tg*Tic20 knockdown on parasite growth further, we performed plaque assays on parental parasites (*D*), knockout parasites (*E*), and knockout parasites complemented with ectopically expressed *Tg*Tic20 (*F*) in the absence (*Upper*) or presence (*Lower*) of ATc. We grew parasites for 9 days in the absence or presence of ATc. During this period, parasites will go through several replication cycles and form zones of clearance (plaques) in the host cell monolayer. We observed a severe growth defect in the presence of ATc in the knockout cell line (*E*, double arrowhead) but not in the parental or complemented lines (*D* and *F*). Arrowheads and double arrowheads depict large and small plaques, respectively.